Desalination and Water Treatment
www.deswater.com
doi: 10.1080/19443994.2013.871349

53 (2015) 2990–2998
March

Taylor & Francis
Taylor & Francis Group

Dynamic adsorption of anionic dyes by apricot shell activated carbon

Julin Cao[a], Yunhai Wu[b,*], Yanping Jin[a], Palizhati Yilihan[a], Shengxin Yang[a]

[a]*College of Environment, Hohai University, Nanjing 210098, China*
[b]*Key Laboratory of Integrated Regulation and Resources Development of Shallow Lakes, Ministry of Education, Hohai University, Nanjing 210098, China*
Tel./Fax: +86 25 83786697; email: wyc0622012@aliyun.com

Received 28 September 2013; Accepted 19 November 2013

ABSTRACT

A continuous adsorption study in fixed-bed columns was investigated using apricot shell activated carbon as an adsorbent for the removal of anionic dyes (Acid Red and Acid Orange II. The effects of the typical column parameters, such as the bed height, influent flow rate, and initial dye concentration, on the breakthrough curves were studied. The increase in bed height resulted in an extension of the breakthrough and exhaustion time, while the increase of both the influent flow rate and initial dye concentration decreased the breakthrough and exhaustion time. The bed depth service time, Bohart–Adams, Yoon–Nelson, and Thomas models were applied to simulate fixed-bed adsorption data and to gain the characteristic parameters of the column. All models were found suitable for describing the whole or a definite part of the dynamic behavior of the column with respect to flow rate and bed height.

Keywords: Apricot shell activated carbon; Anionic dyes; Dynamic adsorption; Fixed-bed column; Breakthrough curve

1. Introduction

Dyes are one of the major constituents of the effluents discharged by various industries including dying, textile, leather, paint, and plastic industry [1]. It is estimated that more than 100,000 commercially available dyes with over 7×10^5 tonnes of dyestuff are produced annually [2]. The presence of these dyes in water is highly visible and affects water transparency, resulting in reduction of light penetration and gas solubility in water, which significantly affects the photosynthetic activity of aquatic plants [3]. As they are generally stable to light, oxidizing agents and resistant to aerobic digestion, many dyes are difficult to degrade [4]. Moreover, investigations have been reported that several of the commonly used dyes, such as Amido Black 10B [5], Bismark Brown R [6], and Congo Red [7], were highly toxic and carcinogenic to human being and aquatic organisms. So, it is essential that the effluents should be treated before discharging dyes into aquatic environments and it has attracted great attention.

Various methods have been developed for dye removal from wastewater, including flocculation [8], ozonation [9], oxidation [10], ion exchange [11],

*Corresponding author.

irradiation [12], biological treatment [13], and adsorption [14]. Among these methods, adsorption technique is quite popular due to its simplicity as well as the availability of a wide range of adsorbents [15]. Activated carbon is the most popular and effective adsorptive material due to its large adsorption capacity, however, its use is limited because of its high cost. Therefore, cheaper substitutes are in great demand. In recent years, cheap and effective adsorbents developed from various waste materials such as eggshell waste [16–18], coconut husk [19], feathers [20,21], bottom ash [22,23], and de-oiled soya [24,25] have been investigated.

In the large number of previous researches, the main focus was put on the adsorption capacities of various adsorbents in batch experiments. However, the data obtained under batch conditions are generally not applicable to most treatment systems where contact time is not sufficient to attain equilibrium [15]. Batch adsorption experiments are usually used for the treatment of small volume of effluents in the laboratory, instead, the continuous adsorption in fixed-bed column is often desired and preferred for industrial application which is simple to operate and can be scaled-up from a laboratory process [26], the experimental data analyzed from the fixed-bed columns provide the most practical application of the dye removal [27].

The objective of this paper was to study the adsorptive removal of anionic dyes, Acid Red (AR), and Acid Orange II (AO), by apricot shell activated carbon (ASAC) in continuous fixed-bed operation. AR and AO belong to hazardous azo dyes, abundantly used in textile industries for dyeing, which could cause serious health problems to humans and animals, and they are carcinogenic in nature [28,29]. In the packed bed experiments, the effects of important factors namely bed height ($Z = 100–300$ mm), influent flow rate ($Q = 10–20$ mL/min), and influent dye concentration ($C_0 = 100–200$ mg/L) on the performance of the column were studied; the results were presented in terms of breakthrough curves. To simulate the breakthrough curves and to determine the characteristic parameters of the column that are useful for process design, four mathematical models: bed depth service time (BDST), Bohart–Adams, Yoon–Nelson, and Thomas models were applied to the experimental data.

2. Materials and methods

2.1. Preparation and characterization of the adsorbent

The untreated ASAC produced from an Active Carbon Ltd. (Jiangsu, China) was used in the study; the carbon was boiled with deionized water for 30 min, then filtered, and dried at 80°C for 24 h. After cooling to room temperature, the carbon was ground and screened through a set of sieves to get different geometrical sizes (40–60 mesh), then stored in a desiccator for further use. Textural characterization of the ASAC was carried out by N_2 adsorption at 77°K using Quantachrome Autosorb-I.

2.2. Dynamic adsorption studies

Column studies were carried out with glass columns of 26 mm inner diameter and 1,000 mm height in which the ASAC wafers were packed. Dye solution of 100, 150, and 200 mg/L was pumped upward through the carbon bed at different flow rates of 10, 15, and 20 mL/min with a peristaltic pump (Masterflex, Cole-Parmer Instrument Co.). Inlet solution pH was kept constant at 4.0 using a JENCO model 6010. Samples were withdrawn from different sampling ports (100, 200, and 300 mm bed height) and measured at regular time intervals. All the experiments were carried out at a constant temperature (25°C).

2.3. Dyes and data analysis

The two anionic dyes were obtained from Nanjing RuiTai chemical reagents Ltd., the structures of AR and AO are shown in Fig. 1. The residual concentration in the effluent was determined using a Shimadzu UV-1201 Spectrophotometer, measuring the absorbance at the maximum wavelength of each dye and being calculated according to the calibration curves. Stock solution (1,000 mg/L) was prepared by dissolving accurately weighed amount of the dye (1 g)

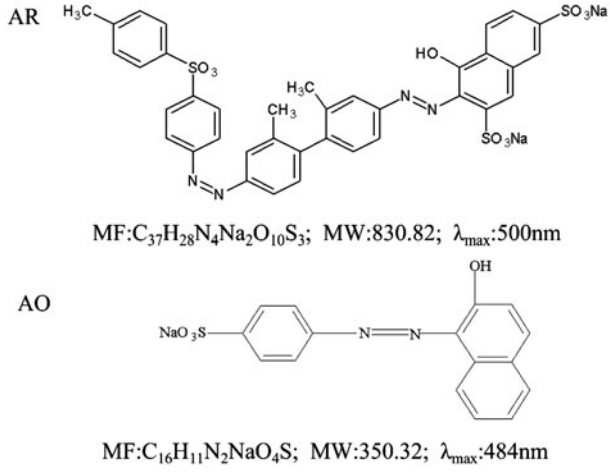

Fig. 1. Chemical structures of the two anionic dyes.

in distilled water. Experimental dye solution of different concentrations was prepared by diluting the stock solution with suitable volume of distilled water. In this study, the breakthrough time was defined as the time when the effluent concentration reached about 5% of the influent concentration, the point where the effluent concentration reached 95% of the influent concentration was called the point of column exhaustion [30].

2.4. Desorption experiment

The regeneration of the adsorbent was performed by using 1 M NaOH, 1 M HNO_3, and 10% ethanol, respectively. The dye-loaded ASAC was separated and stirred with 20 mL of the desorption solutions at 30°C for 4 h on a temperature controlled shaker. After filtration, the adsorbent was washed with deionized water and dried in order to reuse for the next experiment, the dye concentration in the final solution was determined to calculate the desorption efficiency. Consecutive sorption–desorption cycles were repeated three times to establish the reusability of the adsorbent.

All the continuous study experiments were conducted in triplicate within the relative standard deviations limit ±5% and mean values of the results were used in the data analysis [31].

3. Results and discussion

3.1. Characterization of the adsorbent

The density functional theory pore size distribution, BET surface area, and total pore volume were determined from nitrogen adsorption/desorption isotherms measured at −194°C (boiling point of nitrogen gas at atmospheric pressure) [32]. The BET surface area, total pore volume, and average pore diameter of ASAC were found to be 1886.8 m^2/g, 1.31 cm^3/g, and 7.9×10^{-9} m, respectively.

3.2. Effect of the bed height

Breakthrough experiments were carried out with 200 mg/L dye solution and at a flow rate of 20 mL/min at bed heights of 100, 200, and 300 mm at three different runs to study the effect of bed height on breakthrough behavior. From the breakthrough curves obtained, shown in Fig. 2, both the breakthrough and exhaustion time increased with the increasing bed height in the fixed-bed column, the slope of the breakthrough curves of a taller bed is lower than that of a shorter bed. The breakthrough

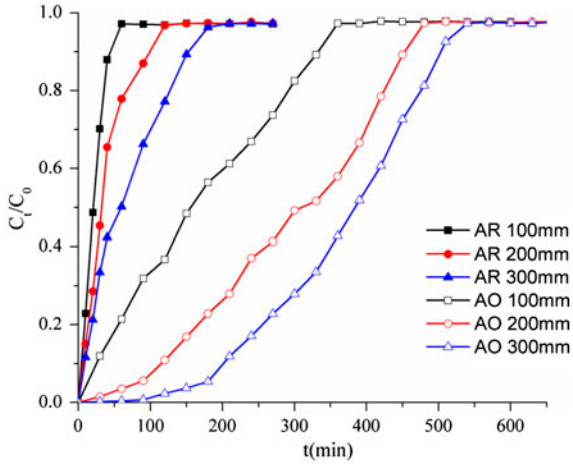

Fig. 2. Breakthrough curves of AR and AO at different bed depths ($C_0 = 200$ mg/L, $Q = 20$ mL/min).

time of AR and AO increased from 3 to 8 min and from 9 to 176 min respectively, for the exhaustion time, AR increased from 60 to 180 min, and AO increased from 354 to 540 min.

The result indicated that the bed depth of 300 mm offered an optimum breakthrough curve for higher uptake. The reason is probably due to that a higher bed height increases the specific surface area of the activated carbon which provided more binding sites for the dye to adsorb [27,33], hence, more liquid could be treated and the breakthrough and exhaustion time are longer [34]. These results were in agreement with those reported in previous studies [35].

3.3. Effect of the influent flow rate

The effect of the influent flow rate was conducted with 200 mg/L dye solution and 300 mm bed height at flow rates of 10, 15, and 20 mL/min. Fig. 3 displays the breakthrough curves at various flow rates of dye solution. As the influent flow rate increased, the breakthrough point in the breakthrough curves moved to the left, the curves became steeper with a shorter mass transfer zone, which meant the bed utilization as well as the bed adsorption capacity reduced. The time required for reaching saturation decreased significantly with an increase in the value of the flow rate.

The breakthrough and exhaustion time decreased as a consequence of the liquid residence time decrease at a higher flow rate [36]. It can be also found that the adsorption capacity was lower at a higher flow rate, due to the insufficient residence time of the solute in the column and the diffusion of the solute into the pores of the adsorbent [37,38]. The reason is that at a

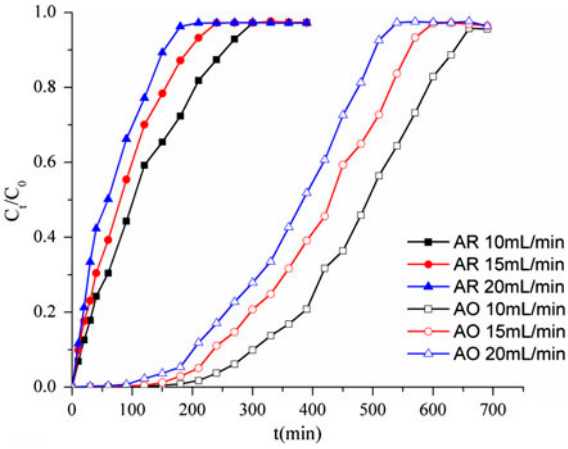

Fig. 3. Breakthrough curves of AR and AO at different influent flow rates (C_0 = 200mg/L, Z = 300 mm).

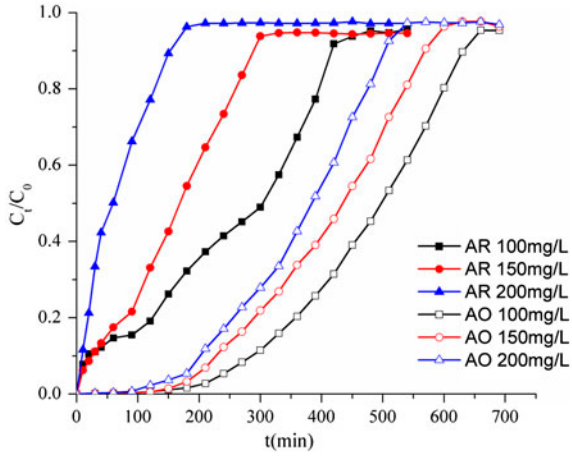

Fig. 4. Breakthrough curves of AR and AO at different initial dye concentrations (Q = 20 mL/min, Z = 300 mm).

higher flow rate, the rate of mass transfer increases, the amount of dye adsorbed onto unit bed height (mass transfer zone) increases with increasing flow rate leading to faster saturation [36,39]. Similar tendency has been found by other researches [40].

3.4. Effect of the initial dye concentration

The experiments were conducted at initial dye concentrations of 100, 150, and 200 mg/L with a flow rate of 20 mL/min and bed height of 300 mm. The shape and the gradient of the breakthrough curves changed significantly, as shown in Fig. 4, which is evident from the breakthrough and exhaustion time decrease with an increase in the initial dye concentration. This may be a consequence of the binding sites becoming more quickly saturated with increasing inlet dye concentration. A lower concentration gradient caused a slower transport due to a decreased diffusion coefficient or decreased mass transfer coefficient [37]. Higher initial concentrations led to higher driving force for mass transfer, hence the adsorbent achieved saturation more fast, which resulted in a decrease of the exhaust time and adsorption zone length [27,41].

3.5. Kinetic models

In order to predict the breakthrough curves of the adsorption process in the fixed bed and estimate the parameters necessary for the design of a large-scale fixed-bed adsorber, the BDST, Bohart–Adams, Yoon–Nelson, and Thomas models have been used.

The BDST model can be used to estimate the required bed depth for a given service-time which is an important parameter in designing an adsorption column [34], the BDST model can be expressed as below [42]:

$$t_b = \frac{N_0}{C_0 U_0}(Z - Z_0) \quad (1)$$

Parameters of the BDST model are shown in Table 1, which could be concluded that the model gave a good fit of the experimental data with the high correlation coefficients ($R^2 > 0.985$ [AR], $R^2 > 0.997$ [AO]). Both the parameters N_0 and Z_0 increased with an increasing in the flow rate shown in Table 1. The thickness of mass transfer zone increases with the flow rate showing the widening of the sorption zone and appearance of a faster breakthrough [42]. The minimum bed depth was obtained at the lowest flow rate as 83.334 mm for AR and 66.063 mm for AO, which was necessary to prevent the effluent concentration from exceeding the breakthrough concentration at zero time.

The Bohart–Adams model is based on the surface reaction theory to describe the relationship between C_t/C_0 and t in a continuous system, which is applied

Table 1
BDST parameters for dye adsorption by ASAC in fixed-bed column at different flow rates (C_0 = 200 mg/L)

Dye	Q (mL/min)	Z_0 (mm)	N_0 (mg/L)	R^2
AR	10	83.334	1.393	0.986
	15	88.875	1.856	0.989
	20	93.912	2.095	0.985
AO	10	66.063	4.163	0.998
	15	71.054	5.142	0.999
	20	92.222	6.291	0.997

to describe the initial part of the breakthrough curve. The Bohart–Adams equation is as follows [43]:

$$\ln\left(\frac{C_0}{C_t}-1\right)=\frac{K_{BA}N_0Z}{U_0}-K_{BA}C_0t \quad (2)$$

The parameters K_{BA} and N_0 can be calculated from the linear plot of $\ln(C_0/C_t-1)$ against t. Different parameters of the Bohart–Adams model were calculated and given in Table 2, the values of K_{BA} increased with an increase of both influent flow rate and bed depth, the values of N_0 increased with increase of the influent flow rate whereas decreased with increasing bed depth. The increase in N_0 can be attributed to the larger mass transfer driving force at high flow rates [44]. With the relatively high coefficients ($R^2>0.976$ [AR], $R^2>0.967$ [AO]) displayed in Table 2, indicating that the Bohart–Adams model was valid for the experimental data. Comparison of the experimental and predicted breakthrough curves obtained at different flow rates and bed heights are given in Fig. 5, which demonstrated that the Bohart–Adams mode is best fitted to low effluent concentrations ($C_t < 0.15C_0$) with a great precision [45].

The Yoon–Nelson model is based on the assumption that the rate of decrease in the probability of adsorption for each adsorbate molecule is proportional to the probability of adsorbate adsorption and the probability of adsorbate breakthrough on the adsorbent [46]. The Yoon–Nelson model for a single component system can be described by the following expression,

$$\ln\frac{C_t}{C_0-C_t}=K_{YN}t-\tau K_{YN} \quad (3)$$

The values of K_{YN} and τ will be obtained from the plot of $\ln[C_t/(C_0-C_t)]$ against t. As seen in Table 3, the K_{YN} increased and the τ decreased with increasing flow rate, while both the K_{YN} and τ increased with increasing bed depth. This was due to the fact that higher flow rate would result in the insufficiency of the adsorption and achieving the adsorption equilibrium early [47]. The data in Table 3 also indicated that the values of τ from the calculation were close to the experimental results. Predicted and experimental breakthrough curves with respect to flow rate and bed height are displayed in Fig. 5, it is clear that there is a good agreement between the experimental and predicted values. Consequently, the Yoon–Nelson model was suitable to describe the adsorption behaviors of ASAC in the column.

The Thomas model is one of the most general and widely used to describe the performance theory of the sorption process in fixed-bed column, which can be commonly used to predict the maximum solute uptake by the adsorbent. This model is suitable for adsorption processes where the external and the internal diffusions will not be the limiting step [48]. The linearized form of this model is given as follows [49]:

$$\ln\left(\frac{C_0}{C_t}-1\right)=\frac{K_{TH}}{Q}q_0m-K_{TH}C_0t \quad (4)$$

The constants, K_{TH} and q_0 were calculated from the slope and intercept of the plot between $\ln[(C_0/C_t)-1]$ vs. t at different flow rates and bed heights. The relative constants and coefficients presented in Table 4 indicated that the Thomas model provided a good fitting at various conditions, as the theoretic uptakes q_0 matched very well with the corresponding experimental data and the determination coefficients were high. It was observed from Table 4 that the values of K_{TH} and q_0 increased with the influent flow rate increasing at constant bed depth. The Yoon–Nelson model was mathematically analogous to the Thomas model, so the fitting results were also quite good (not shown in Fig. 5).

Table 2
Bohart–Adams parameters for dye adsorption by ASAC in fixed-bed column at different bed depths and flow rates ($C_0=200$ mg/L)

Dye	Z (mm)	Q (mL/min)	K_{BA} (L/(mg· min))	N_0 (mg/L)	R^2
AR	100	10	0.000140	1.57	0.986
		15	0.000205	1.93	0.978
		20	0.000475	2.01	0.993
	200	10	0.000100	1.47	0.978
		15	0.000140	1.64	0.987
		20	0.000210	1.75	0.976
	300	10	0.000090	1.50	0.988
		15	0.000110	1.69	0.995
		20	0.000135	1.76	0.987
AO	100	10	0.000050	13.39	0.972
		15	0.000055	14.65	0.973
		20	0.000060	15.30	0.984
	200	10	0.000060	8.18	0.967
		15	0.000065	10.34	0.971
		20	0.000070	10.94	0.969
	300	10	0.000075	6.07	0.989
		15	0.000080	7.93	0.985
		20	0.000085	8.99	0.978

3.6. Desorption and regeneration studies

The regeneration of the adsorbent was studied in order to make the adsorption process more

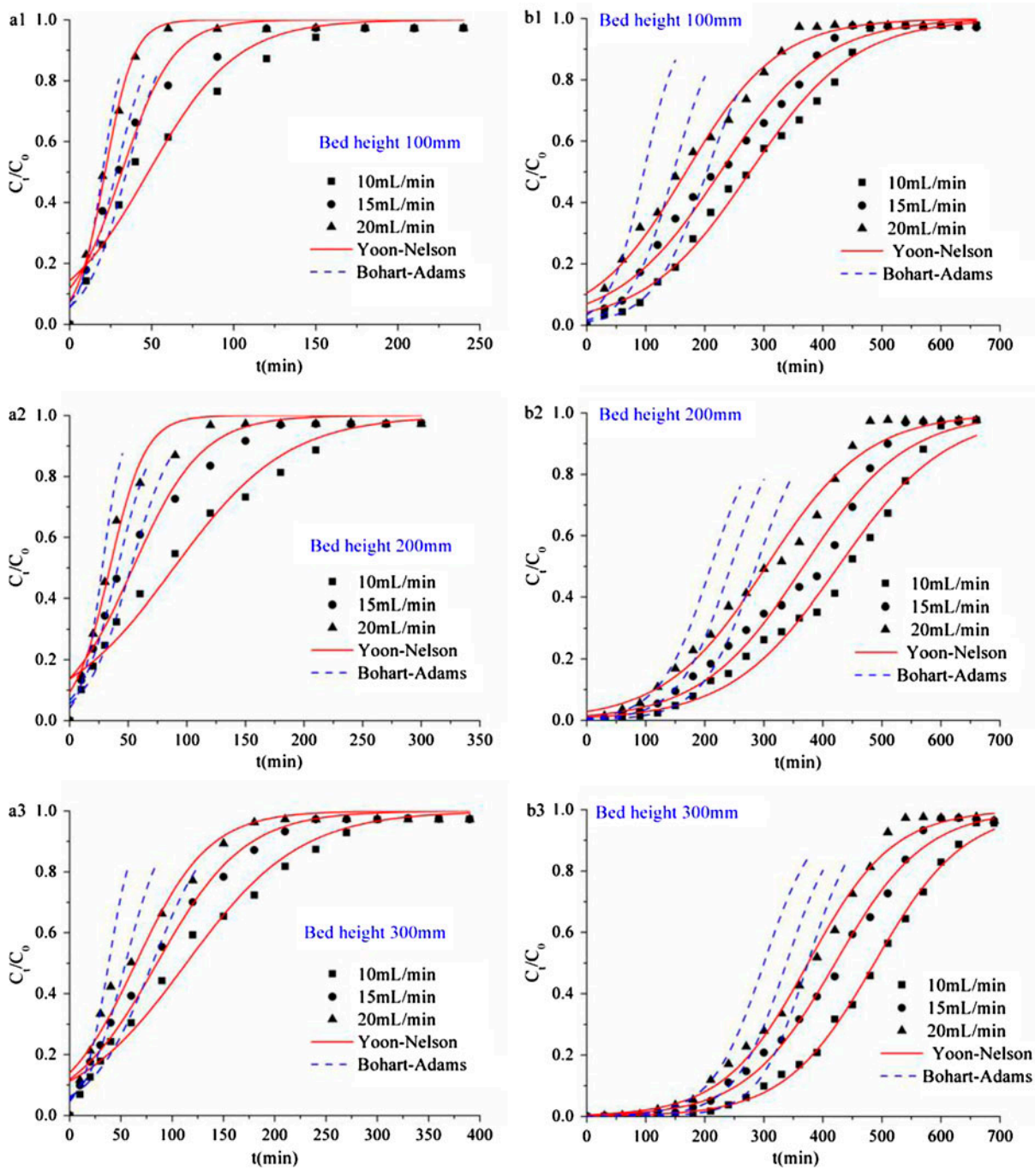

Fig. 5. Comparison of the experimental and predicted breakthrough curves of AR (a) and AO (b) at different flow rates and bed heights.

economical and feasible. It was observed from Fig. 6 that the highest desorption values for AR (69.1%) and AO (53.2%) were obtained using 1 M NaOH solution, while for HNO_3, the desorption efficiencies were 6.35 and 5.72%. The ethanol had a similar low desorption effect on the two dyes. Because the adsorption efficiency was highly dependent on the solution pH, changing the solution pH could easily affect the electrostatic interaction between the adsorbent and dye molecules. After three cycles of regeneration, the

Table 3
Yoon–Nelson parameters for dye adsorption by ASAC in fixed-bed column at different bed depths and flow rates (C_0 = 200 mg/L)

Dye	Z (mm)	Q (mL/min)	K_{YN} (min^{-1})	τ_{cal} (min)	τ_{exp} (min)	R^2
AR	100	10	0.028	47.04	39.85	0.982
		15	0.041	34.05	31.76	0.976
		20	0.095	21.22	20.48	0.993
	200	10	0.021	93.11	86.47	0.975
		15	0.028	54.08	50.25	0.988
		20	0.042	39.10	37.58	0.974
	300	10	0.018	119.11	115.63	0.986
		15	0.022	89.55	85.38	0.991
		20	0.027	66.11	60.21	0.977
AO	100	10	0.011	320.64	295.85	0.978
		15	0.012	248.75	238.63	0.981
		20	0.013	175.08	167.74	0.976
	200	10	0.012	434.25	432.48	0.978
		15	0.013	365.85	373.86	0.986
		20	0.014	290.51	316.27	0.975
	300	10	0.015	483.00	487.24	0.990
		15	0.016	421.13	424.75	0.985
		20	0.017	358.12	376.55	0.979

Table 4
Thomas parameters for dye adsorption by ASAC in fixed-bed column at different bed depths and flow rates (C_0 = 200 mg/L)

Dye	Z (mm)	Q (mL/min)	K_{TH} (mL/(min·mg))	q_0 (mg/g)	q_{exp} (mg/g)	R^2
AR	100	10	0.140	2.087	1.991	0.986
		15	0.205	2.506	2.598	0.978
		20	0.475	2.782	2.903	0.993
	200	10	0.100	2.152	2.039	0.978
		15	0.140	2.284	2.324	0.987
		20	0.210	2.531	2.457	0.968
	300	10	0.090	1.948	2.385	0.988
		15	0.110	1.885	2.299	0.995
		20	0.135	2.284	2.378	0.987
AO	100	10	0.050	17.443	16.689	0.967
		15	0.055	19.082	19.853	0.973
		20	0.060	19.927	20.294	0.984
	200	10	0.060	10.653	10.962	0.963
		15	0.065	13.465	13.165	0.966
		20	0.070	14.286	13.987	0.967
	300	10	0.075	11.717	11.977	0.989
		15	0.080	10.331	10.187	0.985
		20	0.085	11.908	12.178	0.978

adsorption capacity of ASAC decreased by 4.1% for AR and 6.4% for AO. These results indicated the suitability of NaOH as the regenerant for ASAC.

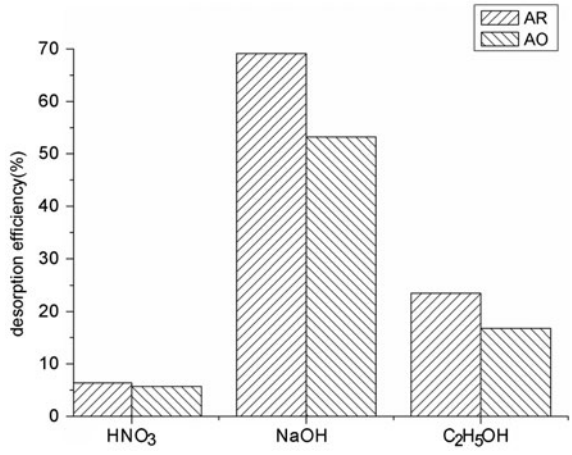

Fig. 6. Desorption efficiencies of dyes from ASAC by various desorbing agents.

4. Conclusions

In the present study, ASAC packed bed has been used to analyze the column dynamics in the adsorption process of removal anionic dyes from aqueous solution. Data confirmed that the breakthrough curves were dependent on the bed depth, influent flow rate, and initial dye concentration. The obtained results showed that both the breakthrough and exhaustion time increased with the increase in the height of the bed, while decreased with the increasing in both the influent flow rate and initial dye concentration. The dynamic behavior of the column was predicted by the BDST, Bohart–Adams, Yoon–Nelson, and Thomas models. All models were found suitable for describing the whole or a definite part of the dynamic behavior of the column with respect to flow rate and bed height. For all studied flow rates and bed heights, the Bohart–Adams model was only used to predict the initial part of the breakthrough curve, while the whole breakthrough curve was well predicted by the Yoon–Nelson and Thomas models. For desorption and regeneration studies, NaOH had been identified as the most effective desorption reagent for the regeneration of ASAC.

Acknowledgment

The authors wish to acknowledge the Hohai University for financial and technical support during this study.

Nomenclature

C_0 — influent liquid concentration of dye (mg/L)
C_t — effluent liquid concentration of dye (mg/L)

K_{BA} — the adsorption rate coefficient of Bohart–Adams model (L/(mg·min))
K_{YN} — the rate constant of Yoon–Nelson model (min^{-1})
K_{TH} — the Thomas model constant (mL/(min·mg))
m — the amount of adsorbent in the column (g)
N_0 — the sorption capacity of the bed per unit bed volume (mg/L)
Q — influent flow rate (mL/min)
q_0 — the adsorption capacity of per unit mass of the adsorbent form Thomas model (mg/g)
R^2 — correlation coefficient
t — the time (min)
t_b — the breakthrough time (min)
U_0 — the fluid velocity (mm/min)
Z — the height of the fixed bed (mm)
Z_0 — the length of the dynamic bed mass transfer zone (mm)
τ — the time required for 50% adsorbate breakthrough from Yoon–Nelson model (min)

References

[1] V.K. Garg, R. Kumar, R. Gupta, Removal of malachite green dye from aqueous solution by adsorption using agro-industry waste: A case study of *Prosopis cineraria*, Dyes Pigm. 62 (2004) 1–10.
[2] J.W. Lee, S.P. Choi, R. Thiruvenkatachari, W.G. Shim, H. Moon, Evaluation of the performance of adsorption and coagulation processes for the maximum removal of reactive dyes, Dyes Pigm. 69 (2006) 196–203.
[3] X.S. Wang, Y. Zhou, Y. Jiang, C. Sun, The removal of basic dyes from aqueous solutions using agricultural by-products, J. Hazard. Mater. 157 (2008) 374–385.
[4] Y.C. Wong, Y.S. Szeto, W.H. Cheung, G. McKay, Equilibrium studies for acid dye adsorption onto chitosan, Langmuir 19 (2003) 7888–7894.
[5] A. Mittal, V. Thakur, V. Gajbe, Adsorptive removal of toxic azo dye Amido Black 10B by hen feather, Environ. Sci. Pollut. Res. 20 (2013) 260–269.
[6] J. Mittal, V. Thakur, A. Mittal, Batch removal of hazardous azo dye Bismark Brown R using waste material hen feather, Ecol. Eng. 60 (2013) 249–253.
[7] A. Mittal, V. Thakur, J. Mittal, H. Vardhan, Process development for the removal of hazardous anionic azo dye Congo red from wastewater by using hen feather as potential adsorbent, Desalin. Water Treat. (2013), doi: 10.1080/19443994.2013.785030.
[8] V. Golob, A. Vinder, M. Simonic, Efficiency of the coagulation/flocculation method for the treatment of dyebath effluents, Dyes Pigm. 67 (2005) 93–97.
[9] M. Muthukumar, N. Selvakumar, Studies on the effect of inorganic salts on decolouration of acid dye effluents by ozonation, Dyes Pigm. 62 (2004) 221–228.
[10] A. Mittal, R. Jain, J. Mittal, S. Varshney, S. Sikarwar, Removal of Yellow ME 7 GL from industrial effluent using electrochemical and adsorption techniques, Int. J. Environ. Pollut. 43 (2010) 308–323.
[11] J. Labanda, J. Sabaté, J. Llorens, Modeling of the dynamic adsorption of an anionic dye through ion-exchange membrane adsorber, J. Membr. Sci. 340 (2009) 234–240.
[12] G. Tezcanli-Güyer, N.H. Ince, Individual and combined effects of ultrasound, ozone and UV irradiation: A case study with textile dyes, Ultrasonics 42 (2004) 603–609.
[13] M. Kornaros, G. Lyberatos, Biological treatment of wastewaters from a dye manufacturing company using a trickling filter, J. Hazard. Mater. 136 (2006) 95–102.
[14] A. El Sikaily, A. Khaled, A. El Nemr, O. Abdelwahab, Removal of Methylene Blue from aqueous solution by marine green alga *Ulva lactuca*, Chem. Ecol. 22 (2006) 149–157.
[15] R.P. Han, D.D. Ding, Y.F. Xu, W.H. Zou, Y.F. Wang, Y.F. Li, L.N. Zou, Use of rice husk for the adsorption of congo red from aqueous solution in column mode, Bioresource Technol. 99 (2008) 2938–2946.
[16] H. Daraei, A. Mittal, M. Noorisepehr, F. Daraei, Kinetic and equilibrium studies of adsorptive removal of phenol onto eggshell waste, Environ. Sci. Pollut. Res. 20 (2013) 4603–4611.
[17] H. Daraei, A. Mittal, J. Mittal, H. Kamali, Optimization of Cr(VI) removal onto biosorbent eggshell membrane: Experimental & theoretical approaches, Desalin. Water Treat (2013), doi: 10.1080/19443994.2013.787374.
[18] H. Daraei, A. Mittal, M. Noorisepehr, J. Mittal, Separation of chromium from water samples using eggshell powder as a low-cost sorbent: Kinetic and thermodynamic studies, Desalin. Water Treat. (2013), doi: 10.1080/19443994.2013.837011.
[19] A. Mittal, R. Jain, J. Mittal, M. Shrivastava, Adsorptive removal of hazardous dye quinoline yellow from waste water using coconut-husk as potential adsorbent, Fresenius Environ. Bull. 19 (2010) 1–9.
[20] A. Mittal, Removal of the dye, Amaranth from waste water using hen feathers as potential adsorbent, Electron. J. Environ. Agric. Food Chem. 5 (2006) 1296–1305.
[21] A. Mittal, J. Mittal, L. Kurup, Utilization of hen feathers for the adsorption of indigo carmine from simulated effluents, J. Environ. Prot. Sci. 1 (2007) 92–100.
[22] V.K. Gupta, A. Mittal, D. Jhare, J. Mittal, Batch and bulk removal of hazardous colouring agent Rose Bengal by adsorption techniques using bottom ash as adsorbent, RSC Adv. 2 (2012) 8381–8389.
[23] J. Mittal, D. Jhare, H. Vardhan, A. Mittal, Utilization of bottom ash as a low-cost sorbent for the removal and recovery of a toxic halogen containing dye eosin yellow, Desalin. Water Treat. (2013), doi: 10.1080/19443994.2013.803265.
[24] A. Mittal, D. Jhare, J. Mittal, Adsorption of hazardous dye Eosin Yellow from aqueous solution onto waste material De-oiled Soya: Isotherm, kinetics and bulk removal, J. Mol. Liq. 179 (2013) 133–140.
[25] A. Mittal, V.K. Gupta, Adsorptive removal and recovery of the azo dye eriochrome black T, Toxicol. Environ. Chem. 92 (2010) 1813–1823.
[26] J.M. Chern, Y.W. Chien, Adsorption of nitrophenol onto activated carbon: Isotherms and breakthrough curves, Water Res. 36 (2002) 647–655.
[27] S.S. Baral, N. Das, T.S. Ramulu, S.K. Sahoo, S.N. Das, G.R. Chaudhury, Removal of Cr(VI) by thermally activated weed *Salvinia cucullata* in a fixed-bed column, J. Hazard. Mater. 161 (2009) 1427–1435.

[28] A. Mittal, L. Kurup, Column operations for the removal and recovery of a hazardous dye 'Acid Red-27' from aqueous solutions, using waste materials–Bottom Ash and De-Oiled Soya, Ecol. Environ. Conservation 12 (2006) 181–186.
[29] V.K. Gupta, A. Mittal, V. Gajbe, J. Mittal, Removal and recovery of the hazardous azo dye acid orange 7 through adsorption over waste materials: bottom ash and de-oiled soya, Ind. Eng. Chem. Res. 45 (2006) 1446–1453.
[30] S. Kundu, S.S. Kavalakatt, A. Pal, S.K. Ghosh, M. Mandal, T. Pal, Removal of arsenic using hardened paste of Portland cement: Batch adsorption and column study, Water Res. 38 (2004) 3780–3790.
[31] M.R.I. Chowdhury, C.N. Mulligan, Biosorption of arsenic from contaminated water by anaerobic biomass, J. Hazard. Mater. 190 (2011) 486–492.
[32] W.T. Tsai, H.C. Hsu, T.Y. Su, K.Y. Lin, C.M. Lin, Removal of basic dye (methylene blue) from wastewaters utilizing beer brewery waste, J. Hazard. Mater. 154 (2008) 73–78.
[33] S. Gupta, B.V. Babu, Modeling, simulation, and experimental validation for continuous Cr(VI) removal from aqueous solutions using sawdust as an adsorbent, Bioresource Technol. 100 (2009) 5633–5640.
[34] H. Muhamad, H. Doan, A. Lohi, Batch and continuous fixed-bed column biosorption of Cd^{2+} and Cu^{2+}, Chem. Eng. J. 158 (2010) 369–377.
[35] Y.S. Al-Degs, M.A.M. Khraisheh, S.J. Allen, M.N. Ahmad, Adsorption characteristics of reactive dyes in columns of activated carbon, J. Hazard. Mater. 165 (2009) 944–949.
[36] D.C.K. Ko, J.F. Porter, G. McKay, Optimised correlations for the fixed-bed adsorption of metal ions on bone char, Chem. Eng. Sci. 55 (2000) 5819–5829.
[37] I.A.W. Tan, A.L. Ahmad, B.H. Hameed, Adsorption of basic dye using activated carbon prepared from oil palm shell: Batch and fixed bed studies, Desalination 225 (2008) 13–28.
[38] A.A. Ahmad, B.H. Hameed, Fixed-bed adsorption of reactive azo dye onto granular activated carbon prepared from waste, J. Hazard. Mater. 175 (2010) 298–303.
[39] W.H. Li, Q.Y. Yue, P. Tu, Z.H. Ma, B.Y. Gao, J.Z. Li, X. Xu, Adsorption characteristics of dyes in columns of activated carbon prepared from paper mill sewage sludge, Chem. Eng. J. 178 (2011) 197–203.
[40] I.A. Aguayo-Villarreal, A. Bonilla-Petriciolet, V. Hernández-Montoya, M.A. Montes-Morán, H.E. Reynel-Avila, Batch and column studies of Zn^{2+} removal from aqueous solution using chicken feathers as sorbents, Chem. Eng. J. 167 (2011) 67–76.
[41] E. Malkoc, Y. Nuhoglu, M. Dundar, Adsorption of chromium(VI) on pomace—An olive oil industry waste: Batch and column studies, J. Hazard. Mater. 138 (2006) 142–151.
[42] O. Hamdaoui, Dynamic sorption of methylene blue by cedar sawdust and crushed brick in fixed bed columns, J. Hazard. Mater. 138 (2006) 293–303.
[43] F.A. Batzias, D.K. Sidiras, Dye adsorption by calcium chloride treated beech sawdust in batch and fixed-bed systems, J. Hazard. Mater. 114 (2004) 167–174.
[44] F. Banat, S. Al-Asheh, R. Al-Ahmad, F. Bni-Khalid, Bench-scale and packed bed sorption of methylene blue using treated olive pomace and charcoal, Bioresource Technol. 98 (2007) 3017–3025.
[45] P. Lodeiro, R. Herrero, M.E. Vicente, The use of protonated *Sargassum muticum* as biosorbent for cadmium removal in a fixed-bed column, J. Hazard. Mater. 137 (2006) 244–253.
[46] S. Kundu, A.K. Gupta, As(III) removal from aqueous medium in fixed bed using iron oxide-coated cement (IOCC): Experimental and modeling studies, Chem. Eng. J. 129 (2007) 123–131.
[47] W.X. Zhang, L. Dong, H. Yan, H.J. Li, Z.W. Jiang, X.W. Kan, H. Yang, A.M. Li, R.S. Cheng, Removal of methylene blue from aqueous solutions by straw based adsorbent in a fixed-bed column, Chem. Eng. J. 173 (2011) 429–436.
[48] Z. Aksu, F. Gönen, Biosorption of phenol by immobilized activated sludge in a continuous packed bed: Prediction of breakthrough curves, Process Biochem. 39 (2004) 599–613.
[49] R.P. Han, W.H. Zou, H.K. Li, Y.H. Li, J. Shi, Copper(II) and lead(II) removal from aqueous solution in fixed-bed columns by manganese oxide coated zeolite, J. Hazard. Mater. 137 (2006) 934–942.